Effects of Surface Chemical Composition on the Early Growth Stages of α-Sexithienyl Films on Silicon Oxide Substrates

Franco Dinelli,* Jean-François Moulin, Maria Antonietta Loi, Enrico Da Como, Massimiliano Massi, Mauro Murgia, Michele Muccini, and Fabio Biscarini

CNR - Istituto per lo Studio di Materiali Nanostrutturati, Bologna Division,Via P. Gobetti 101, I-40129 Bologna, Italy

Jiang Wie and Peter Kingshott

The Danish Polymer Centre, Risoe National Laboratory, Denmark

Received: July 12, 2005; In Final Form: October 26, 2005

In organic field effect transistors, charge transport is confined to a narrow region next to the organic/dielectric interface. It is thus extremely important to determine the morphology and the molecular arrangement of the organic films at their early growth stages. On a substrate of technological interest, such as thermally grown silicon oxide, it has been recently found that α-sexithienyl aggregates made of flat-lying molecules can simultaneously nucleate besides islands made of molecules standing vertical. In this paper, we investigate the effects due to variations in surface chemical composition on α-sexithienyl ultrathin film formation. Flat-lying molecules are no longer detected when Si−OH groups present at the surface are chemically removed but also when the Si−OH or Si−H group density is maximized. This gives evidence that variations in the surface chemical composition can largely affect the nucleation and growth processes of organic/dielectric interfaces. We hypothesize that isolated OH groups can interact with α-sexithienyl molecules and anchor them down flat with respect to the surface.

1. Introduction

The interface formation between an organic semiconductor film and a dielectric surface represents one of the most important issues in organic thin film transistors (OTFT). The accumulation layer, where the charge carriers are capacitively generated, is expected to be confined to a region immediately next to the interface with the gate dielectrics.[1,2] Recently, we have demonstrated that, in the case of orderly grown layered α-sexithienyl (T6) films, the first two monolayers are solely responsible for charge transport.[3] Similar results have been then reported in the case of pentacene[4,5] and dihexyl-quaterthiophene TFTs.[6] It is thus highly relevant to correlate the initial morphology and molecular arrangement of the semiconductor layer to the dielectric surface chemical composition and, eventually, to the film properties.[7]

Studies of organic growth on dielectric surfaces mainly concentrated on films as thick as several tens of monolayers.[8−12] Polymorphism was often observed, but it was not possible to specify the location of the various phases within the films. More recently, the early growth stages have been investigated for the case of T6 on mica[13] and of pentacene on various silicon substrates.[14,15] In particular, T6 is an extensively studied prototype material showing one of the largest charge mobilities among organic semiconductors.[16] Organic molecular beam deposition (OMBD) in ultrahigh vacuum can be controlled to induce a layer-by-layer growth, which is a prerequisite for this type of investigation.[3,13] A very recent study of photoluminescence emission and morphology of submonolayer films grown on thermal silicon oxide has clearly shown that aggregates made of flat-lying molecules can simultaneously nucleate besides monolayer islands made of molecules standing vertical.[17]

Up to now, the influence of substrate chemistry has been only discussed from a phenomenological point of view. Existing models concentrate on 2D vs 3D nucleation as a function of surface energy and generally neglect the possible effects due to molecular anisotropies.[18] Nevertheless, from previous experiments on OTFTs, it was known that hexamethyldisilazane (HMDS) treatment of pristine thermal silicon oxide (t-SiO_2) is essential for improving the electrical performances.[19] In the initial stages of our investigation on the accumulation layer,[3] we have verified that the performances of OTFTs based on T6 directly deposited on t-SiO_2 are also poor in terms of stress (indication of hole traps), contact resistance (nonohmic interface with the electrodes), and mobility values. In particular, charge mobility is typically found $<10^{-3}$ $cm^2/(V\ s)$, that is, more than 10 times less than the values obtained for HMDS-treated t-SiO_2.[3]

In this paper, we specifically focus our attention on the effects induced on the early growth stages of T6 films by variations in the surface chemical composition of silicon oxide substrates. For this purpose, we have employed atomic force microscopy (AFM), transmission electron microscopy (TEM), time-of-flight secondary ion mass spectrometry (TOF-SIMS), and laser scanning confocal microscopy (LSCM).These techniques allow one to map the morphology, molecular arrangement, and chemical composition with high lateral resolution. For submonolayer coverage, it is found that crystalline islands made of nearly vertical molecules always nucleate, independently of the surface chemical composition. In a regime of complete condensation, the activation energy for homogeneous growth

* To whom corresondence should be addressed. E-mail: f.dinelli@bo.ismn.cnr.it. Tel.: +39 051 6398542. Fax: +39 051 6398540.

10.1021/jp053814g CCC: $33.50
Published on Web 12/07/2005

is not strongly affected by large variations in the overall surface properties (namely, hydrophobicity). On the other hand, the nucleation of flat-lying molecule aggregates is found to be dependent on the density of OH groups present at the t-SiO_2 surface, and it is completely suppressed by the removal of OH groups. We believe that this phenomenon might be at the origins of disorder at the boundaries of the first monolayer islands, where hole traps responsible for the electrical performances of devices made on t-SiO_2 can form. Our results are in line with previous publications,[20,21] underlying the crucial role of surface chemical composition on the electrical properties of organic/dielectric interfaces.

2. Experimental

α-Sexithienyl (T6) was synthesized and purified as described in ref 22. Film growth is obtained in an organic molecular beam deposition (OMBD) apparatus with a base pressure of 10^{-10} mbar. The substrate temperature (T_{sub}) can be varied form 25 up to 400 °C and the deposition rate (r) from 10 to <0.02 Å/s.

All the oxide surfaces were cleaned before use by sonication in petroleum ether, dichloromethane, 2-propanol, and water. Thermal and native silicon oxide surfaces were received from CNR-IMM, Bologna, Italy. Hexamethyldisilazane (HMDS) treatment on thermal oxide was carried out in a closed vessel by reaction of the oxide surface with gaseous HMDS. Passivated silicon was prepared by dipping native oxide in 5% HF for 2 min at room temperature, followed by drying with a N_2 flux. Growth of chemical silicon oxide (Si−OH) was performed by dipping passivated silicon in a 30% H_2O_2/NH_4OH 4:1 solution for 10 min at room temperature, followed by rinsing with a 1 mM HCl solution and washing with a copious amount of water.

Contact angle measurements (ultrahigh purity water) were carried out using a DIGIDROP instrument (GBX Instruments). The atomic force microscope (AFM) is a commercial model (Park CP), operated in contact mode as the specimens proved stable enough for imaging under contact.

For TEM analysis, the T6 submonolayer films were transferred to copper electron microscopy grids (200 mesh) using the following flotation technique: we evaporated a thin layer of amorphous carbon on top of the T6 film, put small drops of a polyacrylic acid solution (25% w/w in water, Aldrich) on the zones we wanted to transfer, and then peeled these patches after drying 3−4 h at room temperature. The polyacrylic acid patches were then put upside down on the surface of distilled water and left to dissolve. After 4 h, the self-standing carbon film holding the T6 crystals stripped from the original Si/SiO_x substrate was then fished with copper TEM grids. The samples were observed by bright field electron microscopy and electron diffraction using a Philips CM12 TEM fitted with a LaB6 filament and equipped with an SIS Megaview III CCD camera. The accelerating voltage was 120 kV, and to minimize the beam damage, we constantly used the low dose mode of the microscope together with a small C2 aperture (5−3 μm) and low current (spot 8−9 setting). The selected area electron diffraction patterns were recorded at a 2.50 m chamber length using an aperture of 10 μm.

The laser scanning confocal microscope (LSCM) employed is an inverted Eclipse TE−2000-E Nikon microscope, adapted to perform photoluminescence spectroscopy. A complete description of this experimental setup is reported in ref 23.

The time-of-flight secondary ion mass spectrometry (TOF-SIMS) analysis was performed using a TOF-SIMS IV (Ion-Tof GmbH, Münster, Germany), operated at a pressure of 10^{-8} mbar. A pulsed (15 ns) 25 keV $^{69}Ga^+$ primary ion beam incident at 45° to the surface normal was employed. The mass resolution ($M/\Delta M$) was typically >5000 in positive mode. To achieve high spatial resolution (with a maximum resolution of 250 nm), imaging was performed in the burst alignment mode.[24,25]

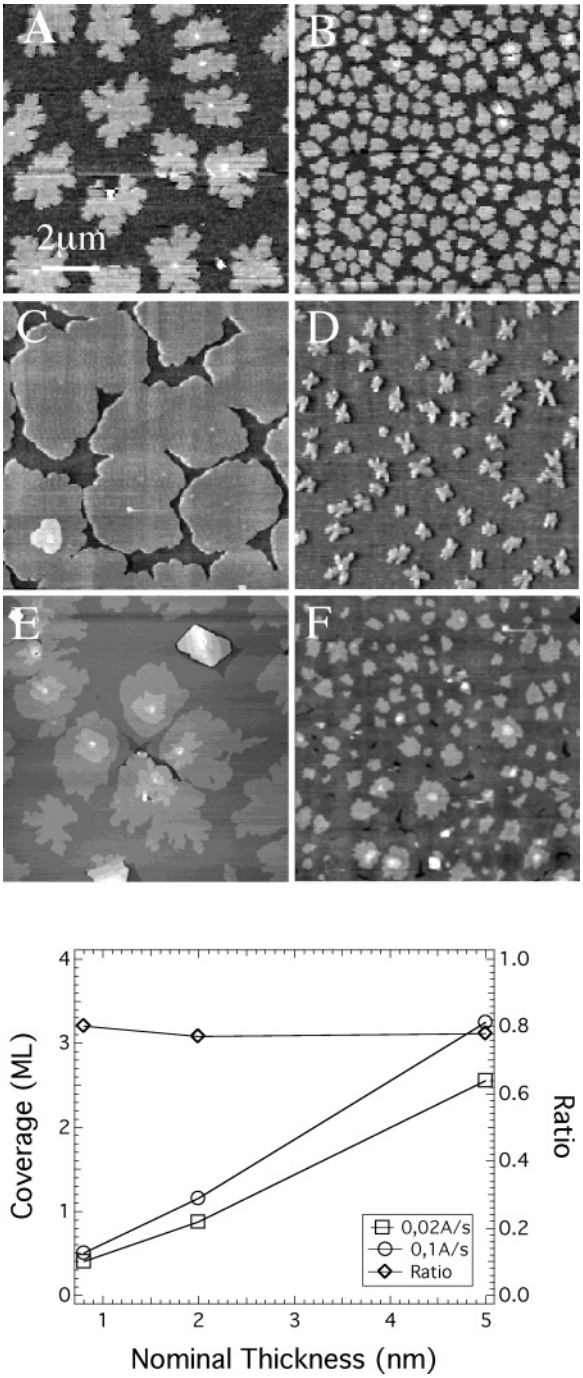

Figure 1. (top) AFM images of films made at 120 °C, 0.02 (left column), and 0.1 Å/s (right column) on t-SiO_2. The total coverage θ ranges from around 0.5 to 3 ML. (bottom) Plot of θ vs nominal thickness t. We have also plotted the ratio between θ obtained at low and high deposition rates.

3. Results

3.1. Ultrathin Film Morphology. In Figure 1, we report AFM topographical images of T6 films deposited on pristine thermal silicon oxide (t-SiO_2) at a T_{sub} of 120 °C and two different r values ($r_1 = 0.02$ and $r_2 = 0.1$ Å/s). The total quantity of material deposited can be evaluated by using a quartz microbalance maintained at room temperature (RT). In the

TABLE 1: List of Substrates Investigated along with Code Names Employed in the Text, Contact Angle Values Measured, and Homogeneous Nucleation Activation Energy E_N Values Evaluated from the Analysis Reported in Figure 3

substrate	code name	contact angle (deg)	E_N (meV)
H-passivated silicon	Si−H	81 ± 2	234 ± 20
pristine thermally grown silicon oxide	t-SiO_2	68 ± 2	244 ± 10
HDMS-treated thermally grown silicon oxide	HMDS/t-SiO_2	70 ± 2	160 ± 10
native silicon oxide	n-SiO_2	26 ± 2	
chemically grown silicon oxide	Si−OH	11 ± 2	252 ± 30

submonolayer regime (parts A and B of Figure 1), the molecules form islands 2.4 ± 0.2 nm high, as estimated by means of AFM.[3] This is evidence that they stand with their long axis almost perpendicular to the substrate. For such a layered structure, the real coverage θ can be defined as the total area covered by the monolayer islands belonging to the first and upper layers. Images reported in Figure 1 represent samples with θ ranging from 0.5 to more than 3 monolayers (ML). As the deposition continues, the island size augments and coalescence eventually occurs until the formation of a complete monolayer (Figure 1C). Then, nucleation of islands 2.4 ± 0.2 nm high, forming the second monolayer, starts and growth proceeds in a layer-by-layer fashion (parts E and F of Figure 1).

In Figure 1 (bottom), θ is plotted vs the total amount of material deposited, expressed in terms of nominal thickness t (assuming a sticking coefficient of 1, a value of 1.4 for the material density and a molecular orientation perpendicular to the substrate plane). At this T_{sub}, desorption is not negligible: for a given t value, r_1 films show lower θ than r_2 films. This has been already reported for other materials, in particular for pentacene.[26] The ratio $\theta_{r_1}/\theta_{r_2}$ is found to be independent from t and equal to 0.8. We can also define the nucleation density N as the number of islands per unit area. In the submonolayer regime (parts A and B of Figure 1), as expected, N increases with increasing r.[27]

T6 films have also been grown on other substrates with different surface chemical composition, namely, chemically grown oxide (Si−OH), thermally grown silicon oxide treated with hexamethyldisilazane (HMDS/t-SiO_2), native silicon oxide (n-SiO_2), and HF-treated silicon (Si−H). Differences in the root-mean-square (rms) roughness of the substrates are negligible: they all range around 0.2−0.3 nm. The hydrophobicity however varies substantially: contact angle data for water are reported in Table 1. A scale of hydrophobicity can be drawn as follows: Si−OH < n-SiO_2 < t-SiO_2 < HMDS/t-SiO_2 < Si−H. Monolayer islands with the same height as those described for t-SiO_2 nucleate on all these surfaces.

For Si−H, Si−OH, and t-SiO_2, we have simultaneously deposited films of fixed t, at 0.04 Å/s and T_{sub} ranging from 25 to 100 °C. In Figure 2, we show the morphology of films grown at 40 and 70 °C. As measured by means of AFM, θ is equal to 0.28 ± 0.01 ML for all substrates. From the power spectrum density of the AFM images, the correlation length ξ can be evaluated.[11,28] At this coverage, assuming that island merging does not yet occur and a narrow island size distribution, ξ represents the average distance between adjacent islands. N can be thus evaluated by making the statistical approximation $N \sim (A/\xi^2)/A = \xi^{-2}$, where A is the area of the image considered and ξ^2 the average area occupied by each island. At 100 °C, desorption becomes non-negligible resulting in a θ reduction

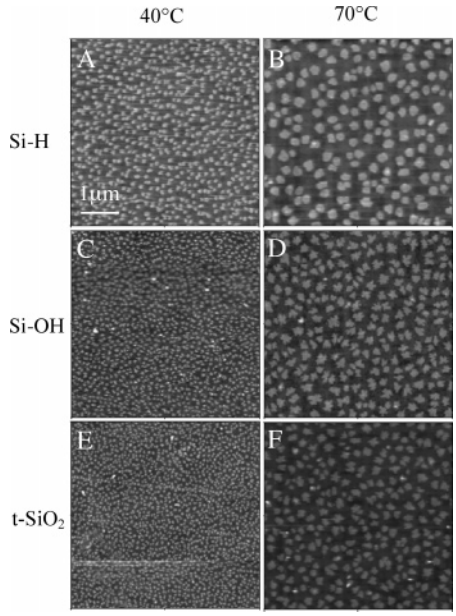

Figure 2. AFM images of films grown on Si−H, Si−OH, and t-SiO_2 at 40 and 70 °C, deposition rate of 0.04 Å/s and 0.28 ML coverage.

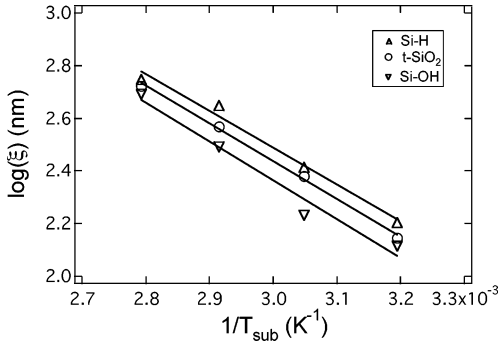

Figure 3. Arrhenius plot of the correlation length ξ vs the substrate temperature T_{sub} (log(ξ) vs log($1/T_{sub}$)) for activation energy E_ξ evaluation.

of roughly 10%. Our analysis is therefore restricted to $T_{sub} \leq$ 85 °C, in a regime of complete condensation.[27]

N turns out to be the highest on Si−OH and the lowest on Si−H. For instance, at T_{sub} = 70 °C, it is equal to 1×10^{-5} nm^{-2} for Si−OH, 7×10^{-6} nm^{-2} for t-SiO_2, and 5×10^{-6} nm^{-2} for Si−H. ξ vs $1/T_{sub}$ is shown as an Arrhenius plot in Figure 3. By fitting the three curves, one obtains the activation energy for homogeneous nucleation $E_N \approx 2 \times E_\xi$. For complete condensation, E_N is equal to $E_d + iE_i$, where E_d represents the diffusion activation energy and E_i the nucleation activation energy of the smallest stable cluster made of i molecules.[27] Data reported in Table 1 indicate that E_N does not vary substantially: Si−H shows the highest, Si−OH the lowest, and t-SiO_2 an intermediate value. From other experiments, HMDS/t-SiO_2 exhibits the smallest E_N value along with the highest nucleation density (Table 1). AFM observations (parts B, D, and F of Figure 2) show that islands formed on Si−H present more round boundaries, whereas islands grown on Si−OH have more fractal boundaries.

For given deposition conditions, the growth of thicker films appears to be independent of the surface chemical composition. Multilayer films can be grown in a nearly layer-by-layer fashion even at room temperature (RT) provided that r is suitably lowered.[3] In Figure 4, we present topographical images of samples grown on Si−H and Si−OH at RT, r < 0.02 Å/s, and θ of several stacked monolayers.

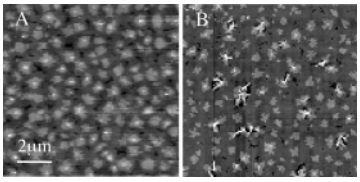

Figure 4. AFM images of layer-by-layer grown films at room temperature on Si−H (A) and Si−OH (B) at a deposition rate of 0.02 Å/s. The total coverage is above 10 ML.

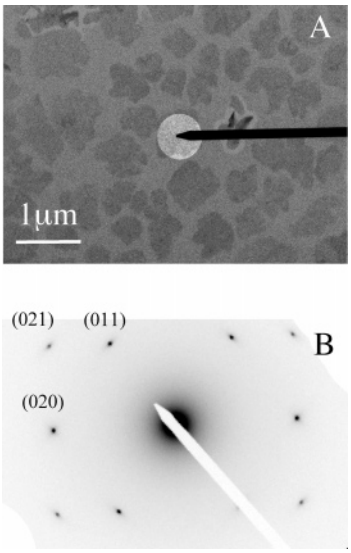

Figure 5. TEM direct image (A) and diffraction pattern (B) of the film region highlighted in (A).

3.2. Molecular Arrangement. On submonolayer samples, we have performed TEM analysis. In Figure 5, we report a representative electron transmission image and the corresponding selected area diffraction pattern recorded on a monolayer island grown on t-SiO_2. The diffraction pattern is characteristic of a single crystal. As we can only observe (0*kl*) spots, only the contact plane of the islands can be deduced. Indexation of the various spots is possible on the basis of a comparison with the bulk structure reported by Horowitz et al.[29] The contact plane turns out to coincide with the *bc* plane of the bulk crystal phase.[30] No noticeable difference was observed between the different substrates at all T_{sub} values investigated. The in-plane orientation of the islands is random, as expected for growth on amorphous isotropic substrates. Therefore, disorder is likely to be present at the island boundaries. However, TEM resolution on these organic samples does not allow us to image such defects as well as defects possibly present within single-crystal islands.

Films grown on Si−H were not studied because their transfer onto TEM grids was not possible by using the method described in the Experimental section. Nevertheless, from grazing incidence X-ray data, we can state that these islands are also crystalline with the same contact plane as those grown on the other substrates.[30]

As previously mentioned, on t-SiO_2, a photoluminescence (PL) emission characteristic of aggregates made of flat-lying molecules has been recently detected.[17] Three regimes can be defined. For θ below 0.04 ML, no PL is ever detectable whereas small monolayer islands already nucleate (as detected by means of AFM). For 0.04 ML $< \theta <$ 1 ML, PL is always detectable in the interstitial areas between monolayer islands. For $\theta >$ 1 ML, no PL has ever been detected suggesting the absence of T6 molecules lying flat. The analysis has been extended to the other substrates under investigation. No such characteristic PL has ever been observed for all T_{sub} values explored from the interstitial areas on Si−H, Si−OH, HMDS/t-SiO_2, and n-SiO_2. Neither AFM operating in contact mode (acquiring frictional force maps) nor in noncontact mode (acquiring phase shift maps) detects the presence of isolated T6 molecules or clusters in the interstitial regions. Therefore, it is not possible to quantify the total amount of material present in the interstices, and in this regime, θ is an underestimation of the real coverage. However, on samples simultaneously grown (Figure 2) showing and not showing PL, there is no appreciable difference in θ within the experimental error. This indicates that the amount of flat-lying molecules is much lower compared to the amount of molecules standing vertical.

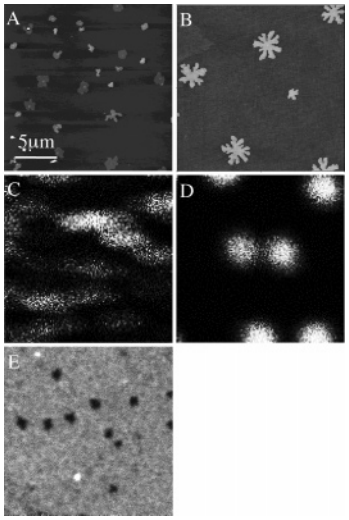

Figure 6. AFM (top row) and TOF-SIMS (second row) images of a submonolayer T6 film deposited on t-SiO_2 (A and C) and n-SiO_2 (B and D). TOF-SIMS images show a chemical map of the S^- ion (*m*/*z* 32): brighter regions denote higher S^- density. The images were acquired in the burst alignment mode (high spatial resolution, low mass resolution). (E) Photoluminescence image of the t-SiO_2 sample: white corresponds to high PL intensity and black to low PL intensity.

TOF-SIMS analysis was performed in order to ascertain that the detection of PL in the submonolayer regime is only due to the presence of T6 molecules in the interstices. In Figure 6, we present AFM and S^- intensity images of samples grown at 150 °C and 0.02 Å/s with 0.3 ML coverage. These samples are suitable for our purpose as the islands are large and well separated (compare with Figure 1). The characteristic PL was observed from the t-SiO_2 sample (Figure 6E) but not from the n-SiO_2 one. The islands made of vertical molecules appear dark as they are not luminescent due to the inefficient coupling between the electric field of the exciting laser and the molecular dipole moment.[17]

Mass spectra were recorded for both samples along with references from bare t-SiO_2, n-SiO_2, and thick T6 films. A complete interpretation of the TOF-SIMS spectra will be reported elsewhere. S^- ions are only generated from the thiophene molecules, thus, the intensity of S^- peaks provides a good contrast between regions where T6 is present or not. Data show that S^- ions are detectable in both the interstitial and island regions on t-SiO_2. On the contrary, no trace of T6 can be detected in the interstitial regions on n-SiO_2, in agreement with PL measurements.

4. Discussion

First, it is worth underlining that monolayer islands with a T6 long axis nearly perpendicular to the surface always nucleate

independently of the surface chemical composition (i.e., whether this is hydrophobic or hydrophilic). These islands are crystalline, and the contact plane coincides with the *bc* plane of the bulk crystal in a wide range of T_{sub}. Both the nucleation density and the island shape change with varying surface chemical composition. The estimated E_N values for homogeneous nucleation differ from 230 to 250 meV (see Table 1). T6 molecules turn out to be more affine to hydrophilic surfaces as further evidenced by the island shape (indicating a higher diffusion around the islands for Si−H). Strikingly, these E_N values obtained in a regime of complete condensation and submonolayer coverage are in close agreement with the value obtained for much thicker films grown on a rather different substrate such as mica (260 meV).[12]

Second, the presence of T6 molecules lying flat on the substrate has been only ascertained for the case of t-SiO_2 in a wide range of deposition conditions. The surface chemical composition of t-SiO_2 is characterized by the presence of Si−O−Si and Si−OH (silanols) groups.[19a,31] The density of OH groups on t-SiO_2 is variable and not controllable.[31] From our data, wafers grown under the same conditions can show contact angle values ranging from 30° to 70°. Variations of up to 30% can also be observed when going from the center to the periphery of the same wafer. After HMDS treatment, the contact angle typically increases, evidence of the removal of OH groups. In the case here presented, the initial high contact angle value indicates that the OH density is rather low. This is further suggested by the small variation in contact angle after the HMDS treatment (Table 1), which fully removes the OH groups. This treatment is sufficient to suppress the presence of aggregates made of flat-lying molecules. It is thus apparent that flat-lying molecule aggregates can only generate in the case of a substrate with an intermediate OH concentration. On the basis of these evidences, we hypothesize that single OH groups can interact with T6 molecules and anchor them down to the surface. Recently, it has been proposed that hydrogen bonds can form between OH groups and S atoms of thiophene rings.[32] This is consistent with our observations and might explain why a high density of OH groups is also detrimental to the phenomenon. A repulsive interaction is likely to occur between the OH groups not interacting with the S atoms and the C atoms of the thiophene rings. Hence, the overall interaction would result repulsive, hampering the molecules from lying flat.

Once anchored, the flat-lying molecules can nucleate stable aggregates in a film with submonolayer coverage.[17] The islands made of standing molecules appear to progressively incorporate the flat-lying molecules during their growth. We can thus infer that they are thermodynamically more stable. On mica, the formation of a stable layer made of molecules lying on their side was on the contrary observed.[13] This molecular reorientation is expected to be an activated process. Depending on T_{sub} and r, defects such as vacancies or dislocations may originate at the boundaries of the randomly oriented islands when they merge. These defects are likely to be in a larger proportion compared to surfaces with high Si−H or Si−OH group densities, where flat-lying molecules are not present and this molecular reorientation does not take place.

Analogous phenomena due to localized substrate/molecule interactions could occur in the early growth stages of other oligomer/dielectric interfaces, also affecting organic/electrode interfaces and device performances. Furthermore, achieving control of supramolecular organization could be crucial in order to exploit other functionalities deriving from molecular anisotropies such as optical ones.[17]

5. Conclusions

Herein, we have presented an investigation of the initial stages of α-sexithienyl film formation on various silicon oxide substrates. In a submonolayer regime, monolayer islands made of molecules standing vertical with respect to the substrate nucleate on all surfaces were investigated. These islands are single crystals with the contact plane coinciding with the *bc* plane independently of the surface chemical composition. The in-plane orientation of different islands is not correlated, and once completed, the first monolayer consists of a mosaic of crystalline domains. The surface chemical composition affects, though slightly, the nucleation density. Hydrophilic surfaces present an activation energy value for homogeneous growth slightly lower with respect to hydrophobic surfaces.

On pristine thermally grown silicon oxide, aggregates made of flat-lying molecules can also nucleate. OH groups present at the surface are likely to anchor the molecules down to the surface. The flat-lying molecules progressively reorient with the completion of the first monolayer. These domains are therefore less stable than the islands formed by vertical molecules. This study provides evidence, for the first time to our knowledge, that variations in the surface chemical composition can largely affect the nucleation and growth processes of organic semiconductors.

Acknowledgment. Authors thank M. Brinkman and M. Schmutz for the use of the TEM facility at the Charles Sadron Institute in Strasbourg, P. Maccagnani for providing thermal and native silicon oxide wafers, and P. Fancello for film growth. This work was supported by EU G5RD-CT2000-00349 MONALISA.

References and Notes

(1) Horowitz, G.; Hajlaoui, R.; Bouchriha, H.; Bourguiga, R.; Hajlaoui, M. *Adv. Mater.* **1998**, *10*, 923.
(2) Dodabalapur, A.; Torsi, L.; Katz, H. E. *Science* **1995**, *268*, 270.
(3) Dinelli, F.; Murgia, M.; Levy, P.; Cavallini, M.; Biscarini, F.; de Leeuw, D. *Phys. Rev. Lett.* **2004**, *92*, 6802.
(4) Ruiz, R.; Papadimitratos, A.; Mayer. A. C.; Malliaras, G. G. *Adv. Mater.* **2005**, *17*, 1795.
(5) Dinelli, F.; Murgia, M.; Biscarini, F.; de Leeuw, D. *Synth. Met.* **2004**, *146*, 373.
(6) Muck, T.; Wagner, V.; Bass, V.; Leufgen, M.; Geurts, J.; Molenkamp, L. W. *Synth. Met.* **2004**, *146*, 317.
(7) Ruiz, R.; Nickel, B.; Koch, N.; Feldman, L. C.; Haglund, R. F.; Kahn, A.; Scoles, G. *Phys. Rev. B* **2003**, *67*, 125406.
(8) Lovinger, A. J.; Davis, D. D.; Dobadalapur, A.; Katz, H. E.; Torsi, L. *Macromolecules* **1996**, *29*, 4952.
(9) Servet, B.; Horowitz, G.; Ries, S.; Lagorsse, O.; Alnot, P.; Yassar, A.; Deloffre, F.; Srivastava, P.; Hajlaoui, R.; Lang, P.; Garnier, F. *Chem. Mater.* **1994**, *6*, 1809.
(10) Lang, P.; Hajlaoui, R.; Garnier, F.; Desbat, B.; Buffeteau, T.; Horowitz, G.; Yassar, A. *J. Phys. Chem.* **1995**, *99*, 5492.
(11) Biscarini, F.; Zamboni, R.; Samorì, P.; Ostoja, P.; Taliani, C. *Phys. Rev. B* **1995**, *52*, 14868.
(12) Biscarini, F.; Samorì, P.; Greco, O.; Zamboni, R. *Phys. Rev. Lett.* **1997**, *12*, 2389.
(13) Muccini, M.; Murgia, M.; Biscarini, F.; Taliani, C. *Adv. Mater.* **2001**, *13*, 355.
(14) Meyer zu Heringdorf, J. F.; Reuter, M. C.; Tromp, R. M. *Nature* **2003**, *412*, 517.
(15) Ruiz, R.; Nickel, B.; Koch, N.; Feldman, L. C.; Haglund, R. F.; Kahn, A.; Family, F.; Scoles, G. *Phys. Rev. Lett.* **2003**, *91*, 136102.
(16) Halik, M.; Klauk, H.; Zschieschang, U.; Schmid, G.; Ponomarenko, S.; Kirchmeyer, S.; Weber, W. *Adv. Mater.* **2003**, *15*, 917.
(17) Loi, M. A.; Da Como, E.; Dinelli, F.; Murgia, M.; Zamboni, R.; Biscarini, F.; Muccini, M. *Nature Mater.* **2005**, *4*, 81.
(18) Veerlak, S.; Steudel, S.; Heremans, P.; Janssen, D.; Deleuze, M. S. *Phys. Rev. B* **2003**, *68*, 5409.
(19) (a) Harstein, A.; Young, D. R. *Appl. Phys. Lett.* **1981**, *38*, 631. (b) Veres, J.; Ogier, S.; Lloyd, G.; de Leeuw, D. *Chem. Mater.* **2004**, *16*, 4543.

(20) Chua, L. L.; Zaumseil, J.; Chang, J.-F.; Ou, E. C.-W.; Ho, P. K.-H.; Sirringhaus, H.; Friend, R. H. *Nature* **2005**, *434*, 194.
(21) Ahles, M.; Schmechel, R.; von Seggern, H. *Appl. Phys Lett.* **2004**, *85*, 4499.
(22) Zamboni, R.; Periasamy, N.; Ruani, G.; Taliani, C. *Synth. Met.* **1993**, *54*, 57.
(23) Loi, M. A.; Da Como, E.; Zamboni, R.; Muccini, M. *Synth. Met.* **2003**, *139*, 687.
(24) Benninghoven, A. *Angew. Chem., Int. Ed. Engl.* **1994**, *33*, 1023.
(25) Vickerman, J. C. *Analyst* **1994**, *119*, 513.
(26) Pratontep, S.; Brinkman, M.; Nuesch, F.; Zuppiroli, L. *Phys. Rev. B* **2004**, *69*, 165201.
(27) Venables, J. A.; Spiller, G. D. T.; Handbucken, M. *Rep. Prog. Phys.* **1984**, *47*, 399.
(28) Barabasi, A.-L.; Stanley, H. E. *Fractal Concepts in Surface Growth*; Cambridge University Press: Cambridge, U.K., 1995.
(29) Horowitz, G.; Bachet, B.; Yassar, A.; Lang, P.; Demanze, F.; Fave, J.-L.; Garnier, F. *Chem. Mater.* **1995**, *7*, 1337.
(30) Moulin, J. F.; Dinelli, F.; Massi, M.; Albonetti, C.; Kshirsagar, R.; Biscarini F. *Nucl. Instrum. Methods Phys. Res*., in press.
(31) Grundner, M.; Graf, D.; Hahn, P. O.; Schnegg, A. *Solid State Technol.* **1991**, *34*, 69.
(32) Chica, A.; Strohmaier, K.; Iglesia, E. *Langmuir* **2004**, *20*, 10952.